THE EUROPEAN
PHYSICAL JOURNAL
SPECIAL TOPICS

Regular Article

Effect of different atmospheres on the synthesis of Ba₂CuGe₂O₇ single crystals

Veronica Granata[1,2,a], Luisa Rocco[1,2], Alberto Ubaldini[2], Martin R. Lees[3], Rosalba Fittipaldi[1,2], Monica Ciomaga Hatnean[3], Sandro Pace[1,2], Geetha Balakrishnan[3], and Antonio Vecchione[1,2]

[1] Dipartimento di Fisica "E.R. Caianiello", Universitá di Salerno, 84084 Fisciano, Salerno, Italy
[2] CNR-SPIN, 84084 Fisciano, Salerno, Italy
[3] Department of Physics, University of Warwick, Coventry CV4 7AL, UK

Abstract. Morphological, compositional and magnetic properties of single crystals of $Ba_2CuGe_2O_7$ grown in oxygen and in dry air have been investigated. It is shown that the use of different atmospheres influences the morphological and compositional characteristics, probably because of some secondary reactions, that occur on the surface of the sample when oxygen is used, but it does not change the structural and magnetic properties. In the case of samples grown in oxygen, a thin, dark superficial layer forms. In this layer impurity particles of $BaCu_2Ge_2O_7$ are present, while the core is formed by pure $Ba_2CuGe_2O_7$.

1 Introduction

A ferroic compound is a material which exhibits a hysteresis cycle of a specific physical property when subjected to an external cyclic stimulus, that can be electric, magnetic or mechanical [1]. For example, a ferroelectric material can acquire a spontaneous electrical polarization that can be reversed by the application of an external electric field. However, the polarization depends not only on the electric field, but also the electric field history.

Those materials which simultaneously show two or more different ferroic orders are called multiferroic and, among them, systems that are instantaneously ferroelectric and ferromagnetic are extremely important and useful for many technological applications. Unfortunately, they are not very common and, indeed, generally ferroelectricity and magnetism are coupled by weak interactions only [2]. For this reason, the research in this field is looking for innovative materials with large coupling.

Among them, such properties are observed in $Ba_2CuGe_2O_7$ (BCGO), that is, indeed, a system particularly intriguing because of its complex magnetic phase diagram [3].

$Ba_2CuGe_2O_7$ crystallizes in the space group $P\bar{4}2_1m$ with a non centrosymmetric tetragonal structure. The lattice parameters are $a = b = 8.466$ Å and $c = 5.455$ Å [4].

---

[a] e-mail: granata@fisica.unisa.it

The structure is formed of Cu–Ge–O layers (where both the germanium and copper ions have tetrahedric coordination with oxygen) separated by planes of Ba^{2+} ions [5].

Cu^{2+} ions ($S = 1/2$) are arranged in a square lattice in the (a, b) plane. Along the [110] direction, nearest-neighbor antiferromagnetic exchange interaction is dominant ($J \leqslant 0.96$ meV per bond), while the ferromagnetic interplane interaction between Cu atoms is weaker ($J_f = -0.026$ meV per bond) [3]. $Ba_2CuGe_2O_7$ is an insulating spiral magnet with an incommensurate structure [6]. Such helimagnetism is due to the presence of a Dzyalonshinskii-Moriya exchange interaction.

Theoretical studies suggest that spiral spin texture and weak ferromagnetism coexist in this material [7] and therefore it is possible that for a narrow range of temperature and magnetic field this material could host a special class of magnetic quasiparticles, the so called skyrmions. Such an idea is supported by recent neutron diffraction experiments that claimed the existence of antiferromagnetic-cone phase [3,8,9]. All these features make $Ba_2CuGe_2O_7$ an extremely interesting material and an useful playground for studies in this field.

In this paper, we report experimental details on the growth of large, defect-free $Ba_2CuGe_2O_7$ crystals by the floating zone method employing two different routes. This method is generally considered a powerful tool for the growth of high purity single crystals of a very large class of materials, including many complex oxides. The quality of the crystals depends on many experimental parameters, such the temperature and the thermal gradient, the translation rate, and the composition. The nature of atmosphere (i.e. its composition and pressure), in which the crystal growth process is performed, also plays an important role. For many different systems, even slight modifications to the growth atmosphere can lead to drastic changes in the physical properties of the samples that are grown.

For instance, in the case of $SrTiO_3$ [10], $CaYAlO_4$ [11], YVO_4 [12] the color of the crystals can be very different if they are grown using different oxygen partial pressure. Sometimes, different colors correspond to different physical properties in materials, making the study of these characteristics even more interesting. For example, stoichiometric ZnO is transparent and a wide band insulator, but very small variations of the Zn-O ratio, make it orange and an n-type semiconductor [13,14], while the stoichiometric NiO is green but a very small oxygen defect makes it black and and a p-type semiconductor [15,16].

There is a huge number of other examples that one could mention, that attest to the importance of controlling the atmosphere and so it should not be surprising that for $Ba_2CuGe_2O_7$ the growth atmosphere can also be a crucial parameter.

Therefore, the effects of different growth atmospheres, oxygen and dried air, on morphological, compositional and structural characteristics are investigated through Scanning Electron Microscopy (SEM), Energy Dispersive Spectroscopy (EDS), Electron backscattering diffraction (EBSD) and X-Ray diffraction. Moreover, magnetization temperature dependence of different samples is discussed.

2 Experimental methods

$Ba_2CuGe_2O_7$ was prepared as polycrystalline powder via a solid solid state reaction by heat treating the starting materials: $BaCO_3$, GeO_2 and CuO, all with purity of at least 99.99%. The details of this process have been reported elsewhere [17]. To prepare the feed rods needed for the crystal growths, these powders were hydrostatically pressed up to 40 MPa in to the form of cylindrical rods. Finally, the polycrystalline $Ba_2CuGe_2O_7$ rods were sintered vertically at 980 °C for 15 h. Growth of single crystals was carried out in a image furnace (NEC Machinery, model SC1-MDH11020) equipped with two 2.0 kW halogen lamps.

To study the effect of oxygen on the crystal properties, growth experiments were performed using different oxygen partial pressure in the range 1–3 bar. As reported in [17] single crystals of $Ba_2CuGe_2O_7$ can be solidified using dry air at 5.5 bar and pure oxygen at 3 bar, corresponding to an oxygen partial pressure of 1.15 and 3 bar, respectively. In the following the samples prepared in this way are referred to as "SAMPLE A" and "SAMPLE B" respectively. Both were grown at a rate of 0.5 mm/h with the feed and seed rods each rotating at 25 rpm in opposite directions.

After the growths were carried out in air and in oxygen, the $Ba_2CuGe_2O_7$ crystals were cleaved along different planes. The crystal surface was investigated by polarized light optical microscopy. Their composition was checked by EDS (Inca, Oxford Instruments) integrated into a SEM (LEO, model EVO 50), for any residual phase, grain boundaries or inclusions.

Some pieces of SAMPLE A and SAMPLE B were ground and checked by X-ray powder diffraction (Bruker D2-PHASER 2nd-generation diffractometer) for phase purity. The instrument works in Bragg-Brentano geometry employing Cu Kα radiation ($\lambda = 1.54$ Å). The data were collected in the 2θ-range from $10°$ to $65°$, using a step size of $0.02°$ and counting time of 10 s for each step. The orientations of naturally occurring facets were determined using Laue diffraction (Photonic Science dual camera system, resolution of 2080×1392 pixels and 12-bit digitisation at 10 MHz) and this Laue system was also used to orient some selected samples for magnetization experiments. Electron backscattering diffraction (Oxford INCA Crystal detector) was also performed to determine the crystallographic orientations of cleaved surfaces. The EBSD patterns were recorded at 20 kV with a working distance of 18.5 mm. The temperature dependence of magnetization was investigated in a Quantum Design, Magnetic Property Measurement System squid magnetometer system in the temperature range 1.5–300 K. The measurements were carried out on SAMPLE A and SAMPLE B, using field cooled mode with an applied magnetic field of 0.1 T.

3 Results and discussion

The XRD patterns of the $Ba_2CuGe_2O_7$ polycrystalline rods are consistent with the expected one and all the peaks have been refined with a $P\bar{4}2_1m$ space group. No evidence of secondary phases was found, proving that this preparation method is effective for the synthesis of this material and that any difference in the crystal boules maybe is due to the different atmosphere used.

Figure 1 shows a picture of SAMPLE A and B crystal boules. We observe that the SAMPLE A, Figure 1a, is pale yellow and nearly perfectly transparent, as generally observed for insulating materials and already found by other groups [9], whereas the SAMPLE B, Figure 1b, appears dark and opaque. Very interestingly, this is not a homogeneous feature of the whole rod. By cutting the sample orthogonal to the growth direction, it was found that a very thin layer (in the following, called "skin") formed on a crystalline "core" with a reddish color, as it can be seen in Figure 1c that shows two cleaved pieces of the inner part of SAMPLES A and B.

A piece of SAMPLE B was cut orthoganal to the growth direction to obtain a surface with a skin-crystal core interface. It was polished and morphological properties were investigated by electron backscattered signal of SEM, to investigate the different areas of the sample. SEM imagines presented some micrometer inclusions (Fig. 2a) close to the edge of cross section that were analyzed by EDS. The inclusions were observed, in average, up to 300 μm from the exterior of the rod, while the core is uniform and no other secondary phases can be observed. While SAMPLE A and areas of SAMPLE B far from the inclusions are very uniform. The inclusions have an excess of copper and a reduced barium content with respect to their value in BCGO
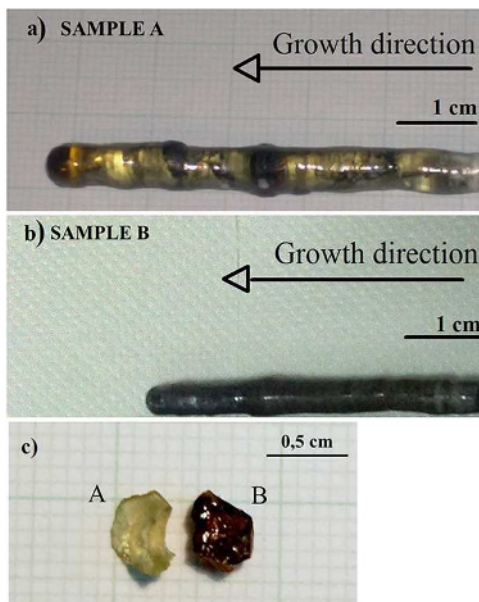
Fig. 1. (a) As-grown single crystal grown in dry air. In this case, there is no dark phase and the sample has a pale yellow color. (b) As-grown single crystal grown in oxygen, showing a dark color. (c) A comparison between a synthesized piece cleaved from a crystal grown in oxygen (on the left) and a piece of crystal grown in dry air (on the right).

Table 1. The results of EDS analysis on SAMPLE A, in the core and on the skin of SAMPLE B.

Sample	Ba (at.%)	Cu (at.%)	Ge (at.%)	O (at.%)
SAMPLE A	15.16	7.69	16.33	54.99
SAMPLE B	15.35	7.62	15.99	52.97
SKIN OF SAMPLE B	11.81	14.4	14.47	47.88

(Figs. 2b and 2c). In contrast the oxygen and germanium were homogeneous everywhere (Figs. 2d and 2e).

To investigate the composition of the crystals, EDS analysis on cleaved SAMPLE A and SAMPLE B and on the skin covering the SAMPLE B were performed. The composition of each crystal, summarized in Table 1, was derived by averaging all EDS data acquired over different areas by normalizing to the stoichiometric value of Ge = 2. The EDS analysis performed on the inclusions shows that the ratio among Ba, Cu and Ge are close to 1:2:2 indicating that these inclusions are mostly made up of $BaCu_2Ge_2O_7$. Similarly, XRD performed on the skin shows evidence for the the presence of this phase. For SAMPLES A and B the ratios of the atoms are almost identical and very closer to the nominal composition, with $Ba_{1.85\pm0.10}Cu_{0.94\pm0.20}Ge_{2.0\pm0.2}O_{6.7\pm0.8}$ and $Ba_{1.9\pm0.1}Cu_{0.9\pm0.2}Ge_{2.0\pm0.2}O_{6.6\pm0.8}$ respectively, while surface covering of SAMPLE B is, on average, much richer in copper. The crystal compositional results were also confirmed by XRD analysis. As expected, the diffraction patterns of SAMPLE A and SAMPLE B (after having carefully removed the skin) show the presence of BCGO only. All the peaks can be indexed and no other phase can be found.
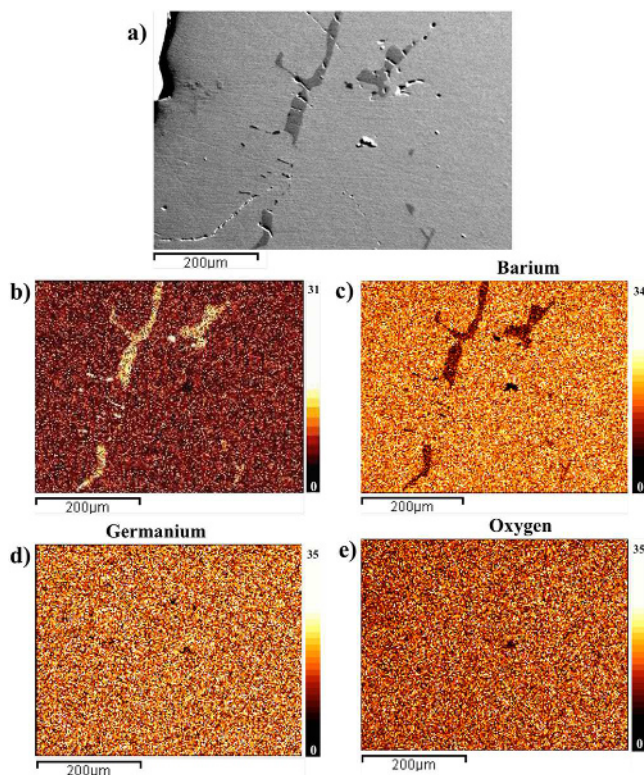
Fig. 2. (a) SEM image of some inclusions present in the skin of SAMPLE B; (b)–(e) EDS compositional maps of the same area. Yellow corresponds to high X-ray intensity (that in turn corresponds to high atomic content of the different elements) and red corresponds to low X-ray intensity (low atomic content).

The powder refinement (Fig. 3) was performed by using Rietveld analysis with FullProf software [18].[1] The refined cell parameters in both cases are in agreement with those already reported [5,19]: $a = 8.470(1)$ Å, $c = 5.446(7)$ Å and $a = 8.469(1)$ Å, $c = 5.447(1)$ Å for SAMPLE A and SAMPLE B respectively. A good agreement is obtained quantitatively supported by a R_p value of 20%, SAMPLE A, and by an R_p value of 18.8%, SAMPLE B, (where R_p factor gives the quality of the fit between simulated and experimental data). These results are comparable with the value of R_p reported in literature [20]. It is worth mentioning that neither type of crystal has a preferred cleavage direction. In Figure 4a EBSD pattern of SAMPLE B shows bright Kikuchi bands [21]. For this technique, a beam of electrons is directed at a point on a tilted $Ba_2CuGe_2O_7$ sample placed in the SEM. A phosphor screen coupled to a Peltier cooled CCD camera is fluoresced by electrons from the sample to form the diffraction pattern [22]. Because the diffraction pattern is bound to the crystal structure of the sample, as the crystal orientation changes the resultant diffraction pattern also changes. The positions of the Kikuchi bands can therefore be used to calculate the orientation of the diffracting crystal using the Hough transform. Kikuchi bands transform to bright regions in Hough space which can be detected and used to calculate the original positions of the bands. Then, the Kikuchi pattern of SAMPLE B is well indexed using the $P\bar{4}2_1m$ space group and the cell parameters determined from
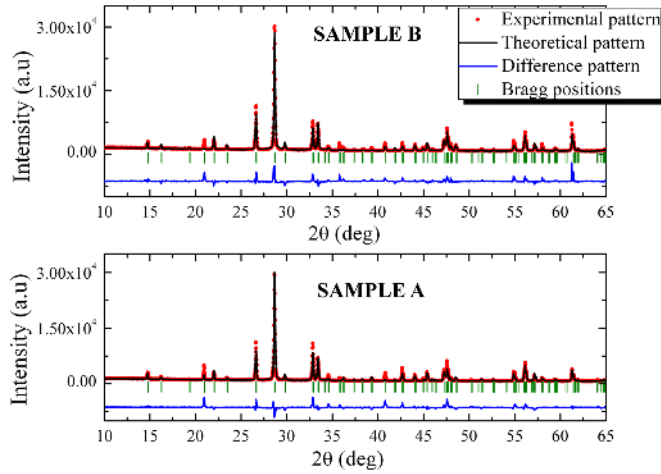
---

[1]Information on https://www.ill.eu/sites/fullprof/index.html

Fig. 3. Simulated diffraction pattern of $Ba_2CuGe_2O_7$ against experimental XRD data of SAMPLES B (top) and A (bottom).

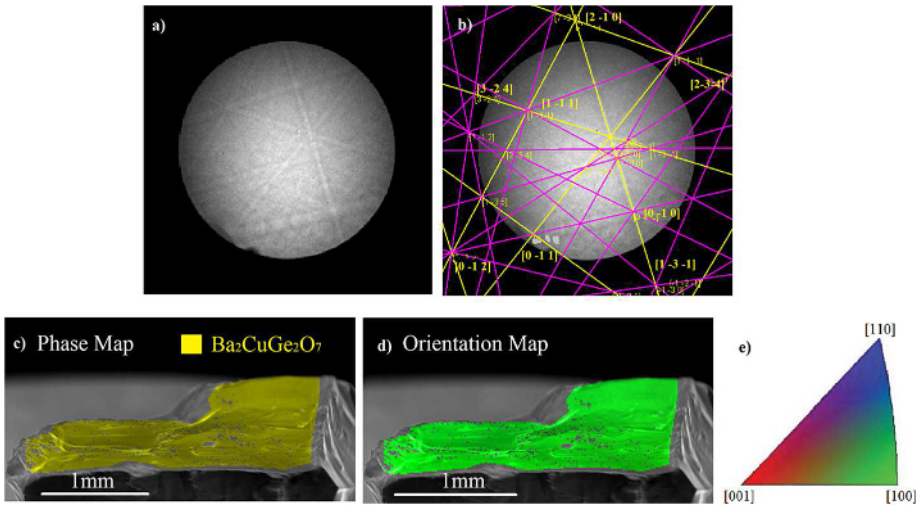**Fig. 4.** (a) and (b) Experimental EBSD pattern and indexed pattern. (c) Phase map on the SEM image of a single $Ba_2CuGe_2O_7$ crystal grown in oxygen (SAMPLE B). The results show that there is only $Ba_2CuGe_2O_7$ phase on analyzed surface. (d) Map of normal orientation to the crystal surface. The sample is oriented with [100] direction orthogonal. (e) Color key of the orientation map.

the XRD. Representative EBSD indexing of the $Ba_2CuGe_2O_7$ is shown in Figure 4b. EBSD micrograph, in good agreement with the other techniques and confirms that $Ba_2CuGe_2O_7$ is the only phase present (Fig. 4c).The diffraction pattern collected on this particular $Ba_2CuGe_2O_7$ sample shows, through the color key, that the [100] or [010] direction is normal to the surface of the analyzed sample (Fig. 4d). We can therefore concluded that the [001] direction lies in the plane of the surface and that the samples are single crystals.

The different color of the crystals A and B, therefore, is not due to major structural or compositional differences, but rather to a slightly smaller band gap for SAMPLE B than for SAMPLE A or, possibly, to the presence impurity levels in the band gap.

In turn, this might be due to very small differences in the oxygen content or possibly to the slightly different cation composition in two samples.

The presence of the skin on SAMPLE B indicates that the growth process follows two different chemical paths. It seems that, in the case of SAMPLE B, a process of partial barium removal takes place, from the outside towards the centre of the sample, because the core is not affected by this phenomenon and its stoichiometry stays constant. The different behavior for SAMPLE A and SAMPLE B likely is due to some different chemical processes, that involve the liquid zone, since the two samples do not show significant differences where the temperature remains lower than the melting point (lower part of the seed rod). Instead, as the temperature in the liquid zone is obviously higher, the chemical activity of elements is greater and it possible that slight direct evaporation of some elements or, eventually, of some of their volatile compounds can occur. It is possible to imagine that a loss of one of these elements happens thanks to a process of formation of some volatile species, inducing the formation of a thin superficial layer, where the chemical composition might be different from the rest of the volume of the liquid. It should be kept in mind that the growth process is very slow and that this removal mechanism may have enough time to induce a local change in the metal concentrations. Among the cations present in this system the most volatile one is barium; its vapor pressure at the melting temperature of BCGO, which is estimated to be around $1000°C$, is about 4 mbar, thus is can not be neglected [23,24]. At the same temperature copper and germanium have vapor pressure around 8.3×10^{-5} mbar [25] and 1.5×10^{-6} mbar [26], respectively. It can thus be argued that the atmosphere surrounding the liquid zone is far richer in barium than in the other two elements. However, the total quantity of these elements in gaseous form might be increased if other volatile compounds form. Considering the composition and pressure of the atmosphere used in the present work, only oxides should be taken into consideration, while other compounds, such as for instance hydroxides, can be neglected because the partial pressure of water in the initial gas is practically zero. Under equilibrium conditions, several oxides may exist in a gaseous form and among them one should find BaO, Ba_2O_3 (that it has been speculated to exist under highly oxidizing conditions, i.e. where the partial pressure of O_2 is several orders of magnitude higher than the partial pressure of $Ba_{(g)}$), CuO, GeO_2 and GeO. In general, their partial pressure at temperatures close to the one at which BCGO grows are quite low (for BaO and CuO at $830°C$ they are around 1.2×10^{-6} mbar and 2.2×10^{-7} respectively [27] and at the same temperature about 1×10^{-6} [28] for GeO_2). Only GeO has a significant partial pressure of about 0.01 mbar [28], but this is still much lower than $Ba_{(g)}$ that is therefore expected to be the most abundant species near the surfaces of the sample rods. In any case, it should be considered that the system under investigation is much more complex than a condensed phase in equilibrium with its vapor, because of the presence of strong thermal gradients and because of the other reactions or different chemical processes that can be involved. For example, the barium evaporation is much stronger from the liquid zone than from the solid parts parts of the rods (feed and growing crystal) that are at much lower temperatures. The gaseous barium can react with oxygen forming barium oxide that, due to the considerations discussed above, is solid and therefore lost to the evaporation equilibrium. The formal chemical equation is:

$$2Ba_{(g)} + O_2 \rightarrow 2BaO_{(s)}. \tag{1}$$
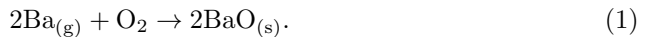
This equation has an associated equilibrium constant, K_p with

$$K_p = P_{Ba}^{-2} \cdot P_{O_2}^{-1} \tag{2}$$

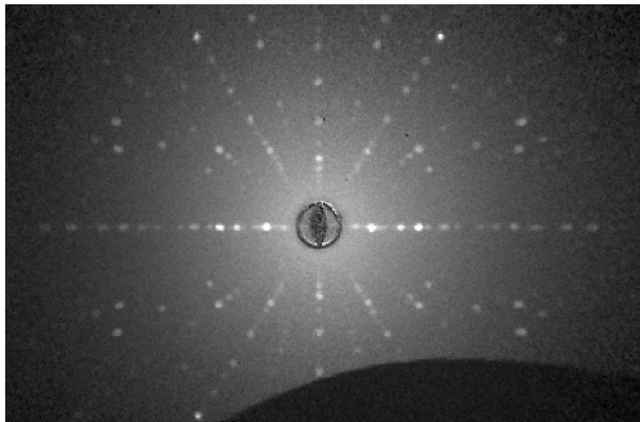**Fig. 5.** X-ray Laue patterns of $Ba_2CuGe_2O_7$ crystal grown in oxygen and oriented with the [010] direction orthogonal to the surface.

where P_{Ba} and P_{O_2} are the partial pressure of barium and oxygen, respectively.

According to this equation, the higher the partial pressure of oxygen, the higher the quantity of BaO forms. Some, likely very small, particles of BaO can form and many of them can fly away from the hot zone, becoming lost for any equilibrium with the liquid sample. Considering that the partial pressure of oxygen is higher for SAMPLE B than for SAMPLE A, (respectively about 3 bar and 1.1 bar), in the former case more BaO should form, forcing greater evaporation of barium from the sample.

While it could be imagined that, in most of the liquid volume, the homogenization and the feeding of new material from the melting feed can prevent the formation of important concentration gradients, in proximity of the liquid-crystal growth interface it is possible that this evaporation can lead to the appearance of a barium poor area. Actually near the interface the temperature is lower and the viscosity increases [29,30] and so the diffusion becomes less effective. The gradient can therefore survive. Thus, according to this hypothesis, the local composition moves away from the stoichiometric composition required for the BCGO crystallization, and an excess of copper and germanium is found. This excess, in turn, leads to the precipitation of the inclusions, found in the skin. Locally, the composition becomes close to that of the $BaCu_2Ge_2O_7$ phase that therefore form preferentially. The precipitation does not occur in the case of SAMPLE A, because of the less oxidizing conditions, for which much less barium is subtracted from the equilibrium vapor–liquid. In this instance, there is no reason for the formation of the barium poor layer because the driving force for this process is absent.

However, regardless these the processes involved during the solidification, the crystal quality of the SAMPLES A and B is similar. In fact the Laue diffractometry of SAMPLE B (Fig. 5) is similar to the one of crystals grown in dry air as reported in [17]. This means that the crystallization is not affected by what happens on the surface of the sample suggesting that the solidification process starts from the center of the rods. Actually there is no direct information about the radial thermal gradient that exists in the liquid and near the interface between it and the growing crystal, but it is possible that the core can be just slight cooler than the surface and so the nucleation of begins from the center. Considering the samples are very similar in terms of composition and structure, it is not surprising that their magnetic properties are also quite similar. The magnetization as function of temperature of SAMPLE A and SAMPLE B was taken by using a magnetic field parallel to the cleaved plane, is
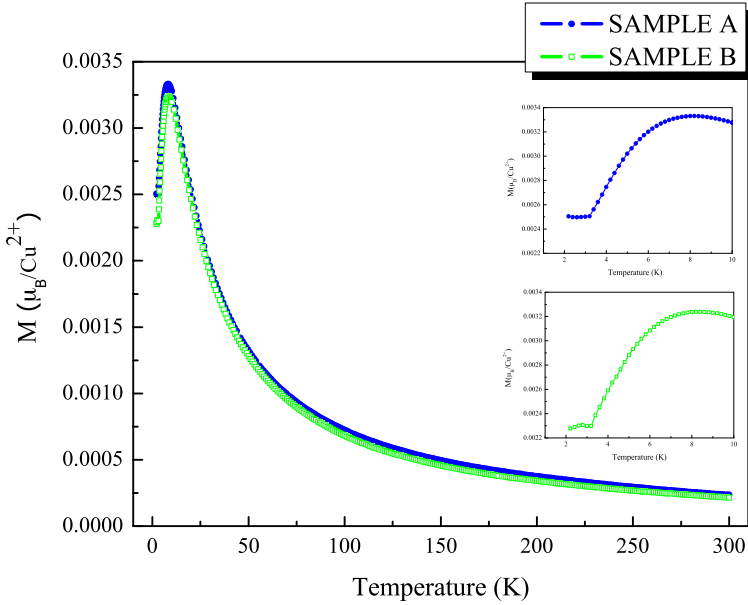
Fig. 6. Magnetization versus temperature of $Ba_2CuGe_2O_7$ single crystals for a field $\mu_0 H = 0.1\,T$ applied parallel to the [101] direction.

shown in Figure 6. Both samples present a broad maximum in their magnetization curves centered at $T \sim 8.5\,K$ and an inflection at $T_N \sim 3.3\,K$ are observable. This behavior is in agreement with the results already reported in literature [6]. The magnetization below $T = 3\,K$ is explained with an in plane antiferromagnetic order [31]. The observation that the signal in SAMPLE A is slightly higher that in SAMPLE B may be due to very small difference in the oxygen content in the two samples.

4 Conclusions

$Ba_2CuGe_2O_7$ single crystals were grown in different atmospheres, 3 bar of pure oxygen or 5.5 bar of dry air, by the floating zone technique. It is shown that these atmospheres have some influences on the growth of this material.

$Ba_2CuGe_2O_7$ crystal boule grown in dry air is transparent and yellow in color, while the single crystal boule grown in oxygen is reddish and is covered in a thin, dark, surface layer.

The composition of the all samples was investigated by EDS and X-ray diffraction analysis. The samples grown under oxygen have some inclusions in the first 300 μm surface layer. EDS and X-ray diffraction have shown that these inclusions are composed of a $BaCu_2Ge_2O_7$ phase. The composition of cleaved pieces of the core of SAMPLE B (without inclusions) is very similar to the sample grown under air (SAMPLE A). This suggests that in the former case, a barium removal process acts locally. Very likely this process is due to an evaporation of barium in addition to a strong oxidation to Barium oxide due to highly oxidizing conditions. The Rietveld refinement shows that SAMPLE A and SAMPLE B have the same expected crystalline structure. Magnetic properties were also investigated and the different samples exhibit the paramagnetic behavior reported in literature.

In conclusion, we can confirm that the crystals grown in oxygen without inclusions have a dark color and they show crystalline structure and magnetic properties comparable with the measurements in the literature. Further analysis are required to understand the different optical properties and possible different bands structures of these samples.

References

1. N.A. Spaldin, M. Fiebig, Science **309**, 391 (2005)
2. S.W. Cheong, M. Mostovoy, Nat. Mater. **6**, 13 (2007)
3. S. Mühlbauer, S. Gvasaliya, E. Ressouche, E. Pomjakushina, A. Zheludev, Phys. Rev. B **86**, 024417 (2012)
4. M. Tovar, R. Dinniebier, W. Eysel, Mater. Sci. Forum **278**, 750 (1998)
5. A. Zheludev, S. Maslov, G. Shirane, Phys. Rev. B **57**, 2968 (1998)
6. A. Zheludev, G. Shirane, Y. Sasago, N. Kiode, K. Uchinokura, Phys. Rev. B **54**, 15163 (1996)
7. A.N. Bogdanov, M. Wolf, K.-H. Muller, Phys. Rev. B **66**, 214410 (2002)
8. A. Zheludev, S. Maslov, G. Shirane, Phys. Rev. B **59**, 11973 (1999)
9. S. Mühlbauer, S.N. Gvasaliya, E. Pomjakushina, A. Zheludev, Phys. Rev. B **84**, 180406(R) (2011)
10. P.I. Nabokin, D. Souptel, A.M. Balbashov, J. Cryst. Growth **250**, 397 (2003)
11. W. Wan, X. Yan, X. Wu, Z. Zhang, B. Hu, J. Zhou, J. Cryst. Growth **219**, 56 (2000)
12. S. Erdei, F. Ainger, Mater. Res. Soc. Symp. Proc. **329**, 245 (1993)
13. R. Raji, K.G. Gopchandran, J. Sci.: Adv. Mater. Devices **2**, 51 (2017)
14. A.B. Djurišić, Y.H. Leung, K.H. Tam, L. Ding, W.K. Ge, H.Y. Chen, S. Gwo, Appl. Phys. Lett. **88**, 103107 (2006)
15. A. Renaud, B. Chavillon, L. Cario, L. Le Pleux, N. Szuwarski, Y. Pellegrin, E. Blart, E. Gautron, F. Odobel, S. Jobic, J. Phys. Chem. C **117**, 22478 (2013)
16. B. Sasi, K.G. Gopchandran, P.K. Manoj, P. Koshy, P. Prabhakara Rao, V.K. Vaidyan, Vacuum **68**, 149 (2002)
17. R. Fittipaldi, L. Rocco, M. Ciomaga Hatnean, V. Granata, M.R. Lees, G. Balakrishnan, A. Vecchione, J. Cryst. Growth **404**, 223 (2014)
18. R.A. Young, in *The Rietveld Method*, IUCr Monographs on Crystallography (Oxford University Press, Oxford, U.K., 1993), Vol. 5.
19. V. Granata, A. Ubaldini, R. Fittipaldi, L. Rocco, S. Pace, A. Vecchione, J. Cryst. Growth **457**, 128 (2017)
20. M. Sun, A.E. Nelson, J. Adjaye, J. Phys. Chem. B **110**, 2310 (2006)
21. A.J. Schwartz, M. Kumar, B. Adams, *Electron Backscatter Diffraction in Material Science* (1980)
22. A.J. Wilkinson, P.B. Hirsch, Micron **28**, 279 (1997)
23. E. Rudberg, J. Lempert, J. Chem. Phys. **3**, 627 (1935)
24. K.T. Jacob, Y. Waseda, J. Less Common Metals **139**, 249 (1988)
25. H. N. Hersh, J. Am. Chem. Soc. **75**, 1529 (1953)
26. A.W. Searcy, J. Am. Chem. Soc. **74**, 4789 (1952)
27. T. Sata, K. Sakai, S. Tashiro, J. Am. Ceram. Soc. **74**, 1445 (1991)
28. L. Zhang, Z. Xu, J. Hazard. Mater. **312**, 28 (2016)
29. S.W. Strauss, Nucl. Sci. Eng. **12**, 436 (1962)
30. G. Wu, E. Yazhenskikh, K. Hack, E. Wosch, M. Müller, Fuel Process. Technol. **137**, 93 (2015)
31. H. Murakawa, Y. Onose, S. Miyahara, N. Furukawa, Y. Tokura, Phys. Rev. B **85**, 174106 (2012)